MEASURING AND UTILIZING GRAVITY-GRADIENT INDUCED TORQUES ON FUTURE GRAVITY RECOVERY MISSIONS

Ryan Kinzie*, Riccardo Bevilacqua†, Dongeun Seo‡, Huaizu You§, John W. Conklin¶ and Peter J. Wass‖

This research is a novel investigation into the use of newly-available relative angular acceleration measurements between a spacecraft utilized for gravity recovery missions and an internally located test mass. The gravity-gradient torque equation for zonal spherical harmonic order n is formulated for a known gravitational potential field, and through simulations it is proven that the Simplified-Gravitational Reference Sensor will be sensitive to the gravity-gradient induced torques acting on its test mass. This research then demonstrates how the presented gravity-gradient torque equation and the measured relative angular acceleration between the spacecraft and test mass will improve the accuracy of the gravity field models acquired by future gravity recovery missions by directly measuring the drag acting on the spacecraft with a single accelerometer.

INTRODUCTION

Starting in 2002 the Gravity Recovery and Climate Experiment (GRACE) mission measured the temporal variations of Earth's gravity field caused by the transport of masses and their redistribution in the Earth system.[1] Several years after the beginning of the GRACE mission, the Gravity Field and Steady-State Ocean Circulation Explorer (GOCE) spacecraft was launched with the objective of improving the accuracy and spatial resolution of Earth's gravity field maps measured by GRACE.[1] The GOCE mission accomplished this by using a 6-component gradiometer, which was comprised of six three-axis precision accelerometers. The gradiometer allowed the spacecraft to directly measure the drag acting on the GOCE spacecraft and the gravity-gradient tensor (second derivative of the gravitational potential).[2] Following the end of the GRACE mission in 2017, the Gravity Recovery and Climate Experiment Follow-On (GRACE-FO) mission began in 2018. The accelerometers utilized in the GRACE, GOCE and GRACE-FO mission were all built by Office

*Graduate Student, Department of Aerospace Engineering, AIAA Student Member, Embry-Riddle Aeronautical University, Daytona Beach, FL 32114, USA, Email: kinzier@my.erau.edu

†Interim Associate Dean and Professor, Department of Aerospace Engineering, AIAA Associate Fellow, Embry-Riddle Aeronautical University, Daytona Beach, FL 32114, USA, Email: bevilacr@erau.edu

‡Associate Professor, Department of Aerospace Engineering, AIAA Member, Embry-Riddle Aeronautical University, Daytona Beach, FL 32114, USA, Email: seod@erau.edu

§Guidance Navigation and Control Systems Lead and Systems Engineer, Attitude Control Systems Engineering Branch (Code 5910) and Mission Systems Engineering Branch (Code 5990), NASA Goddard Spaceflight Center, Greenbelt, MD 20771, USA, Email: huaizu.you@nasa.gov

¶Associate Professor, Department of Mechanical and Aerospace Engineering, University of Florida, Gainesville, FL 32611, USA, Email: jwconklin@ufl.edu

‖Research Scientist, Department of Mechanical and Aerospace Engineering, University of Florida, Gainesville, FL 32611, USA, Email: pwass@ufl.edu

National d'Etudes et Recherches Aérospatiales (ONERA) and consist of a test mass electrostatically suspended in a vacuum surrounded by six pairs of sensing and actuation electrodes.[3] Since there are six pairs of sensing and actuation electrodes there is the potential for the accelerometers to measure the simultaneous 6-axis relative acceleration measurements (3-axis translation and 3-axis angular) of the host spacecraft with respect to the test mass.

Although the GOCE accelerometer had the potential to measure the relative angular acceleration, only the relative translational acceleration measurements were utilized to measure the drag and gravity-gradient tensor.[2] Similarly, only the relative translational acceleration measurements are utilized in the current version 04 release of the GRACE-FO level 1-A and level 1-B data products.[4] In the case of the GRACE-FO mission, the relative angular acceleration measurements from the ONERA accelerometer are instead replaced by angular acceleration estimations of the GRACE-FO spacecraft which are computed from a Kalman filter that uses star tracker, IMU and magnetorquer measurements as inputs.[3] The reason for replacing the measured relative angular acceleration with the estimated angular acceleration of the spacecraft is attributed to the noise of the accelerometer and its insensitivity to gravity-gradient induced torques on the test mass under normal operating conditions.[4] Although the estimations computed by the Kalman filter have been shown to be less noisy and more accurate than the measurements from the accelerometer, the estimations are only available for the spacecraft angular acceleration, not the relative angular acceleration between the spacecraft and test mass. Using the spacecraft angular acceleration instead of the relative acceleration potentially excludes useful gravity recovery data, the main observable for the GRACE-FO mission. Although it is unlikely that the gravity-gradient induced torques on the test mass will ever be observable to the GRACE-FO accelerometer, we believe that these torques will be observable to the Simplified Gravitational Reference Sensor's (S-GRS) accelerometer which is estimated to be up to 500 times more sensitive than the GRACE accelerometers and 5 times more sensitive than the GOCE accelerometers.[1,5] The S-GRS is an ultra-precise inertial sensor for future Earth geodesy missions currently being developed by the University of Florida and houses an accelerometer in addition to laser ranging equipment. The S-GRS's accelerometer is illustrated in Figure 1 and consists of a test mass electromagnetically suspended in a vacuum surrounded by seven pairs sensing and actuation electrodes.

In 2019 as part of the Decadal Survey for Earth Science, the Mass Change Applications Team found that most practical applications require an increase to the temporal and spacial resolutions and the accuracy of the spherical harmonic coefficients and functions of the currently available gravity field maps.[6] As stated by the Committee on Earth Gravity from Space,[7] this is of significant interest to many fields of study including ocean dynamics, continental water variation, sea-level rise, post-glacial rebound, structure and evolution of the earth's crust and lithosphere, and mantle dynamics. Kornfeld et al.[8] have identified the major sources of error for the GRACE-FO mission, which lists drag modeling errors as a main contributor to the error of the estimated geopotential parameters. However, Behzadpour et al.[9] state that it is not possible to model the drag accurately for the GRACE-FO mission. Therefore, in addition to presenting the sensitivity of the S-GRS's accelerometer to the gravity-gradient torques acting on its test mass, this research also demonstrates how the newly available data may be utilized to directly measure the drag on a GRACE-FO type gravity recovery mission. To the extent of the authors' knowledge, no previous research has investigated the connection between gravity recovery scientific data and the relative angular acceleration between a host spacecraft and its test mass.

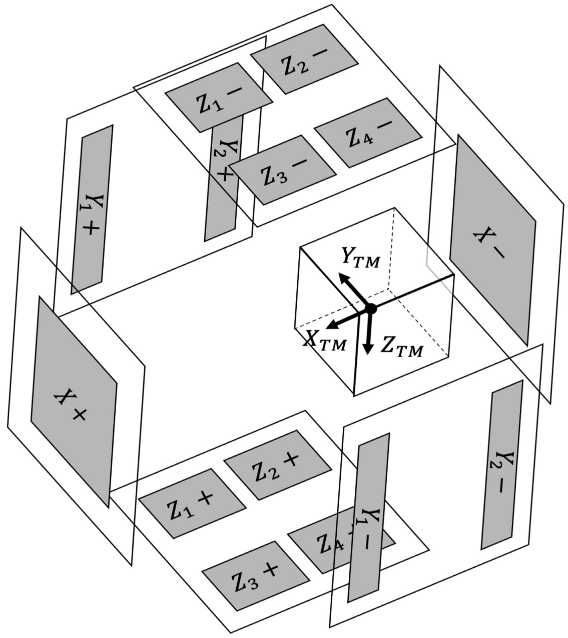

Figure 1. S-GRS's Test Mass with Sensing and Actuation Electrodes

The rest of this paper is organized as follows; the Formulation section explains the frames that are referenced throughout this paper and formulates the gravity-gradient torque equation for zonal spherical harmonic degree n. Additionally, this section presents the algorithm for directly measuring the drag on a gravity recovery spacecraft when a minimum of two accelerometers are present, and presents the derivation of how a single S-GRS accelerometer may directly measure the drag acting on the same spacecraft. The Simulation section then presents the sensitivity of the S-GRS to the relative angular acceleration between the GRACE-FO spacecraft and the S-GRS's test mass and simulates the two accelerometer algorithm and the single accelerometer algorithm. Finally, the Discussion and Conclusion sections of this paper compare the two algorithms and state the achievements of this research.

FORMULATION

In this section, the reference frames are presented followed by the equations used to model the gravity-gradient torque due to zonal spherical harmonic degree n for a known gravitational potential field. The algorithm for directly measuring the drag on a gravity recovery spacecraft when a minimum of two accelerometers is also presented, which is followed by the derivation for a single accelerometer.

Frame Definition

For this research, a test mass is placed inside of a low-Earth-orbiting spacecraft. Therefore, three frames are utilized; the Inertial Frame (denoted with I), the Body-Fixed Frame (denoted with B), and the Test Mass Frame (denoted with TM). The Inertial Frame is the defined as the canonical Earth-Centered Inertial (ECI) coordinate frame. The Body-Fixed Frame is defined the same way that the Satellite Frame and the Science Reference Frame are defined in the GRACE-FO Level-1

Data Product User Handbook,[10] with origin of the Body-Fixed Frame attached to the center-of-mass of the spacecraft. Finally, the Test Mass Frame originates at the center-of-mass of the test mass where the x-axis is ram pointing, the z-axis is nadir pointing, and the y-axis follows from the right-hand rule. All three frames are presented in Figure 2, where a single GRACE-FO spacecraft is illustrated. In Figure 2, $\bar{r}_{TM/B}$ denotes the position of the Test Mass Frame with respect to the Body-Fixed Frame, and $\bar{r}_{B/I}$ and $\bar{r}_{TM/I}$ denote the position of the Body-Fixed Frame and the Test Mass Frame with respect to the Inertial Frame, respectively.

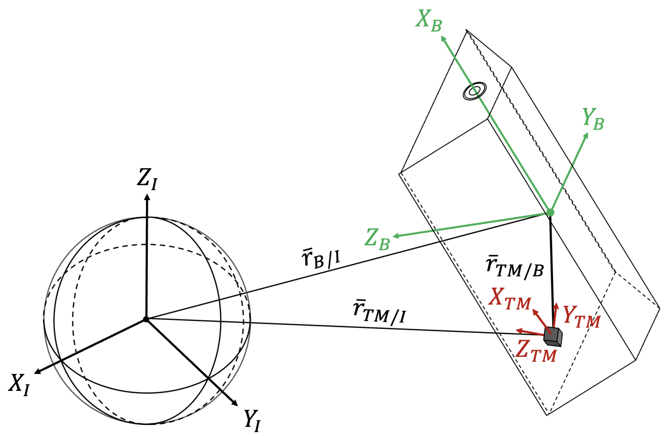

Figure 2. Frames of Reference. The Inertial Frame (I), Body-Fixed Frame(B) and Test Mass Frame (TM) are illustrated along with their respective position vectors

Gravity-Gradient Torque

When the gravitational potential U (the negative of the potential energy) is known, its respective gravity-gradient tensor, G_{J_n}, may be used to model the gravity-gradient torque, $\bar{\tau}_{\nabla g}$, on the spacecraft for J_n zonal spherical harmonics,[11]

$$(\bar{\tau}_{\nabla g})^{\times} = \left(G_{J_n} I^B\right)^T - G_{J_n} I^B \tag{1}$$

Here, I^B is the moment of inertia of the spacecraft and the superscript $\times$ denotes the skew-symmetric operator. The gravity-gradient tensor for zonal spherical harmonic degree n and its relation to the gravitational potential follow as the matrices,[12]

$$G_{J_n} = \begin{bmatrix} \frac{\partial^2 U}{\partial x^2} & \frac{\partial^2 U}{\partial x \partial y} & \frac{\partial^2 U}{\partial x \partial z} \\ \frac{\partial^2 U}{\partial y \partial x} & \frac{\partial^2 U}{\partial y^2} & \frac{\partial^2 U}{\partial y \partial z} \\ \frac{\partial^2 U}{\partial z \partial x} & \frac{\partial^2 U}{\partial z \partial y} & \frac{\partial^2 U}{\partial z^2} \end{bmatrix} = \begin{bmatrix} \frac{\partial g_{x,n}}{\partial x} & \frac{\partial g_{x,n}}{\partial y} & \frac{\partial g_{x,n}}{\partial z} \\ \frac{\partial g_{y,n}}{\partial x} & \frac{\partial g_{y,n}}{\partial y} & \frac{\partial g_{y,n}}{\partial z} \\ \frac{\partial g_{z,n}}{\partial x} & \frac{\partial g_{z,n}}{\partial y} & \frac{\partial g_{z,n}}{\partial z} \end{bmatrix}$$

Note that $\bar{a}_{J_n} = [g_{x,n}, g_{y,n}, g_{z,n}]^T$ is the transitional gravitational acceleration vector. The gravity-gradient tensor is symmetric since $\frac{\partial g_{x,n}}{\partial y}$, $\frac{\partial g_{y,n}}{\partial x}$ both lie on the spacecraft's xy-plane, $\frac{\partial g_{x,n}}{\partial z}$, $\frac{\partial g_{z,n}}{\partial x}$ on the xz-plane and $\frac{\partial g_{y,n}}{\partial z}$, $\frac{\partial g_{z,n}}{\partial y}$ on the yz-plane. G_{J_n} may be solved for discretely if we assume that,

$$\frac{\partial g_{x,n}}{\partial x} \approx \frac{\Delta g_{x,n}}{\Delta x} = \frac{g_{x_1,n} - g_{x_2,n}}{x_1 - x_2} \tag{2}$$

where $g_{x_1,n}$ and $g_{x_2,n}$ are discrete gravitational acceleration measurements made at the known locations, x_1 and x_2, respectively. Similarly we can say that, $\frac{\partial g_{x,n}}{\partial y} \approx \frac{\Delta g_{x,n}}{\Delta y}$, $\frac{\partial g_{x,n}}{\partial z} \approx \frac{\Delta g_{x,n}}{\Delta z}$, $\frac{\partial g_{y,n}}{\partial y} \approx \frac{\Delta g_{y,n}}{\Delta y}$, $\frac{\partial g_{y,n}}{\partial z} \approx \frac{\Delta g_{y,n}}{\Delta z}$ and $\frac{\partial g_{z,n}}{\partial z} \approx \frac{\Delta g_{z,n}}{\Delta z}$. Using Eq. (2) and considering only the symmetric elements of $(\bar{\tau}_{\nabla g})^{\times}$, relation between the discrete acceleration measurements and the gravity-gradient torques can be derived with the help of Eq. (2) as follows,

$$\bar{\tau}_{\nabla g} = \mathcal{H}\left(I^B, \Delta\bar{x}\right) \times \Delta\bar{a}_{J_n} = \begin{bmatrix} -I_{xx}\frac{1}{\Delta x} - I_{xy}\frac{1}{\Delta y} - I_{xz}\frac{1}{\Delta z} \\ -I_{yy}\frac{1}{\Delta y} - I_{yz}\frac{1}{\Delta z} - I_{xy}\frac{1}{\Delta x} \\ -I_{zz}\frac{1}{\Delta z} - I_{xz}\frac{1}{\Delta x} - I_{yz}\frac{1}{\Delta y} \end{bmatrix} \times \Delta\bar{a}_{J_n} \tag{3}$$

where $\Delta\bar{x} = [\Delta x, \Delta y, \Delta z]^T$ and where $\Delta\bar{a}_{J_n} = [\Delta g_{x,n}, \Delta g_{y,n}, \Delta g_{z,n}]^T$ are n^{th} order acceleration measurements.

Accelerometer Measurements

Since the electrode housing of the S-GRS's accelerometer is rigidly connected to the spacecraft the accelerometer will measure the relative translational and angular acceleration between its test mass and the spacecraft. To find an expression for the relative translational acceleration measurements, the translational acceleration of the S-GRS's test mass is first considered,

$$\begin{aligned} \bar{a}^B_{TM/I} = \left(\bar{a}^B_{TM/I}\right)_{Earth} + \bar{\alpha}^B_{B/I} \times \bar{r}^B_{TM/B} + \bar{\omega}^B_{B/I} \times \left(\bar{\omega}^B_{B/I} \times \bar{r}^B_{TM/B}\right) \\ + 2\bar{\omega}^B_{B/I} \times \bar{v}^B_{TM/B} + \left(\bar{a}^B_{TM/I}\right)_{other} \end{aligned} \tag{4}$$

Here, $\left(\bar{a}^B_{TM/I}\right)_{Earth}$ is the translational acceleration acting on the test mass resulting from Earth's gravity, $\bar{\alpha}^B_{B/I} \times \bar{r}^B_{TM/B}$, is the Euler acceleration due to the angular acceleration of the spacecraft and the position offset of the test mass relative to the spacecraft center-of-mass, $\bar{\omega}^B_{B/I} \times \left(\bar{\omega}^B_{B/I} \times \bar{r}^B_{TM/B}\right)$ is the centripetal acceleration due to the angular velocity of the spacecraft and the test mass offset and $2\bar{\omega}^B_{B/I} \times \bar{v}^B_{TM/B}$ is the Coriolis acceleration of the test mass with respect to the spacecraft's center-of-mass. Additionally, it is important to note that the superscripts I, B, TM, denote whether the respective vector is resolved in either the Inertial, Body-Fixed or Test Mass Frames, respectively. Finally, $\left(\bar{a}^B_{TM/I}\right)_{other}$ denotes all other translational accelerations acting on the test mass such as the acceleration which results from the spacecraft - test mass coupling, which is a force that is exerted on the test mass that is generated by the spacecraft's changing gravitational and magnetic field.[13] Here, it is assumed that the spacecraft's attitude is controlled and the position of the test masses from the spacecraft's center-of-mass are reasonably small. Therefore the Euler, centripetal and Coriolis accelerations are negligible[2] and will not appear in the rest of the derivation.

The translational acceleration of the spacecraft is now considered, and is a summation of the acceleration acting on the spacecraft due to Earth's gravity $\left(\bar{a}^B_{B/I}\right)_{Earth}$, the acceleration due to drag $\left(\bar{a}^B_{B/I}\right)_{drag}$ and the all other nongravitational accelerations $\left(\bar{a}^B_{B/I}\right)_{other}$ which result from external forces such as Earth radiation pressure, solar radiation pressure, etc.

$$\bar{a}^B_{B/I} = \left(\bar{a}^B_{B/I}\right)_{Earth} + \left(\bar{a}^B_{B/I}\right)_{drag} + \left(\bar{a}^B_{B/I}\right)_{other} \tag{5}$$

The measured relative translational acceleration between the test mass and spacecraft is found by subtracting Eq. (5) from Eq. (4),

$$\bar{a}^B_{TM/B} = \left(\bar{a}^B_{TM/I}\right)_{Earth} - \left(\bar{a}^B_{B/I}\right)_{Earth} - \left(\bar{a}^B_{B/I}\right)_{drag} + \left(\bar{a}^B_{TM/I}\right)_{other} - \left(\bar{a}^B_{B/I}\right)_{other}$$

The above equation will be simplified slightly by setting $\left(\bar{a}^B_{TM/B}\right)_{other} = \left(\bar{a}^B_{TM/I}\right)_{other} - \left(\bar{a}^B_{B/I}\right)_{other}$ for notation convenience,

$$\bar{a}^B_{TM/B} = \left(\bar{a}^B_{TM/I}\right)_{Earth} - \left(\bar{a}^B_{B/I}\right)_{Earth} - \left(\bar{a}^B_{B/I}\right)_{drag} + \left(\bar{a}^B_{TM/B}\right)_{other} \tag{6}$$

To derive an expression for the relative angular acceleration measurements, the angular acceleration of the S-GRS's test mass is considered,

$$\bar{\alpha}^B_{TM/I} = \left(\bar{\alpha}^B_{TM/I}\right)_{Earth} + \left(\bar{\alpha}^B_{TM/I}\right)_{other} \tag{7}$$

Here, $\left(\bar{\alpha}^B_{TM/I}\right)_{Earth}$ is the angular acceleration acting on the test mass due to Earth's gravity gradient torque and $\left(\bar{\alpha}^B_{TM/I}\right)_{other}$ is the angular acceleration due to all other forces acting on the test mass, such as the angular acceleration that is generated from the spacecraft - test mass coupling. Similarly, the angular acceleration of the spacecraft will be the summation angular acceleration acting on the spacecraft due to Earth's gravity gradient torque $\left(\bar{\alpha}^B_{B/I}\right)_{Earth}$, the angular acceleration resulting from drag $\left(\bar{\alpha}^B_{B/I}\right)_{drag}$ and the all other nongravitational angular accelerations which result from external forces acting on the spacecraft $\left(\bar{\alpha}^B_{B/I}\right)_{other}$,

$$\bar{\alpha}^B_{B/I} = \left(\bar{\alpha}^B_{B/I}\right)_{Earth} + \left(\bar{\alpha}^B_{B/I}\right)_{drag} + \left(\bar{\alpha}^B_{B/I}\right)_{other} \tag{8}$$

Subtracting Eq. (8) from Eq. (7) yields the measured relative angular acceleration between the test mass and spacecraft,

$$\bar{\alpha}^B_{TM/B} = \left(\bar{\alpha}^B_{TM/I}\right)_{Earth} - \left(\bar{\alpha}^B_{B/I}\right)_{Earth} - \left(\bar{\alpha}^B_{B/I}\right)_{drag} + \left(\bar{\alpha}^B_{TM/I}\right)_{other} - \left(\bar{\alpha}^B_{B/I}\right)_{other}$$

The above equation will be simplified slightly for notation convenience by setting $\left(\bar{\alpha}^B_{TM/B}\right)_{other} = \left(\bar{\alpha}^B_{TM/I}\right)_{other} - \left(\bar{\alpha}^B_{B/I}\right)_{other}$,

$$\bar{\alpha}^B_{TM/B} = \left(\bar{\alpha}^B_{TM/I}\right)_{Earth} - \left(\bar{\alpha}^B_{B/I}\right)_{Earth} - \left(\bar{\alpha}^B_{B/I}\right)_{drag} + \left(\bar{\alpha}^B_{TM/B}\right)_{other} \tag{9}$$

Solving For Drag

In this subsection two methods for solving for the drag using the S-GRS's accelerometer will be presented. The first method assumes there are a minimum of two accelerometers onboard the spacecraft, and the second method may be applied when only a single S-GRS accelerometer is present (any number of S-GRS accelerometers may be present).

Two Accelerometers When two accelerometers are present the drag acting on the spacecraft may be solved for by using a derivation similar to the one presented in Cesare.[2] If the derivation is done correctly, the drag on the spacecraft will be equal to,

$$\left(\bar{a}^B_{B/I}\right)_{drag} = \frac{1}{2}\left(\left(\bar{a}^B_{TM1/B}\right)_{other} - \bar{a}^B_{TM1/B}\right) + \frac{1}{2}\left(\left(\bar{a}^B_{TM2/B}\right)_{other} - \bar{a}^B_{TM2/B}\right) \tag{10}$$

where $TM1$ and $TM2$ denote the first and second test masses, respectively, and $\left(\bar{a}^B_{TMi/B}\right)_{other} = \left(\bar{a}^B_{TMi/I}\right)_{other} - \left(\bar{a}^B_{B/I}\right)_{other}$ with $i = 1, 2$. It is important to note the this method only utilizes the translational acceleration measurements which allowed this method to be implemented on the GOCE mission.[2]

One S-GRS Accelerometer When only one S-GRS accelerometer is present the derivation to solve for the drag acting on the spacecraft is more involved and is one of the major innovations of this research. The derivation begins by taking advantage of the fact that $\bar{\tau} = \bar{x} \times \bar{F}$ where $\bar{\tau}$ is torque and $\bar{x}$ is the position of the force, $\bar{F}$, with respect to the spacecraft's center-of-mass. The torque acting on the spacecraft due to drag is therefore,

$$\left(\bar{\tau}^B_{B/I}\right)_{drag} = \bar{x}_{Cp/B} \times \left(\bar{F}^B_{B/I}\right)_{drag} \tag{11}$$

where $\left(\bar{F}^B_{B/I}\right)_{drag}$ is the drag force and $\bar{x}_{Cp/B}$ is the position of the spacecraft's center-of-pressure with respect to the spacecraft's center-of-mass,

$$\bar{x}_{Cp/B} = \frac{S_1\bar{x}_{c_{p_1}} + S_2\bar{x}_{c_{p_2}} + \ldots + S_n\bar{x}_{c_{p_n}}}{S_1 + S_2 + \ldots + S_n}$$

Here, S_n is the cross-sectional area of the n^{th} panel and $\bar{x}_{c_{p_n}}$ is the n^{th} position of the center-of-pressure with respect to the spacecraft's center-of-mass. Since $\left(\bar{F}^B_{B/I}\right)_{drag} = m^B\left(\bar{a}^B_{B/I}\right)_{drag}$ where m^B is the mass of the spacecraft and $\left(\bar{\tau}^B_{B/I}\right)_{drag} = I^B\left(\bar{\alpha}^B_{B/I}\right)_{drag}$, the angular acceleration of the spacecraft due to drag may be solved for from Eq. (11),

$$\left(\bar{\alpha}^B_{B/I}\right)_{drag} = m^B\left(I^B\right)^{-1}\bar{x}_{Cp/B} \times \left(\bar{a}^B_{B/I}\right)_{drag} \tag{12}$$

Utilizing Eq. (3) the angular accelerations acting on the test mass and spacecraft due to Earth's gravity gradient torque in Eq. (9) are equivalent to,

$$\left(\bar{\alpha}^B_{TM/I}\right)_{Earth} = \left(I^{TM}\right)^{-1}\mathcal{H}\left(I^B, \Delta\bar{x}_{TM,B}\right) \times \left[\left(\bar{a}^B_{TM/I}\right)_{Earth} - \left(\bar{a}^B_{B/I}\right)_{Earth}\right]$$

and,

$$\left(\bar{\alpha}^B_{B/I}\right)_{Earth} = \left(I^B\right)^{-1}\mathcal{H}\left(I^B, \Delta\bar{x}_{TM,B}\right) \times \left[\left(\bar{a}^B_{TM/I}\right)_{Earth} - \left(\bar{a}^B_{B/I}\right)_{Earth}\right]$$

where I^{TM} is the mass of the test mass. Substituting the above equations and plugging Eq. (12) into Eq. (9) yields,

$$\begin{aligned}\bar{\alpha}^B_{TM/B} = &\left[\left(I^{TM}\right)^{-1} - \left(I^B\right)^{-1}\right]\mathcal{H}\left(I^B, \Delta\bar{x}_{TM,B}\right) \times \left(\bar{a}^B_{TM/I}\right)_{Earth} \\ &- \left[\left(I^{TM}\right)^{-1} - \left(I^B\right)^{-1}\right]\mathcal{H}\left(I^B, \Delta\bar{x}_{TM,B}\right) \times \left(\bar{a}^B_{B/I}\right)_{Earth} \\ &- m^B\left(I^B\right)^{-1}\bar{x}_{Cp/B} \times \left(\bar{a}^B_{B/I}\right)_{drag} + \left(\bar{\alpha}^B_{TM/B}\right)_{other}\end{aligned} \tag{13}$$

Operation	**Action**
Addition	$a + b = \left[a_0 + b_0, \left(\bar{a} + \bar{b}\right)^T\right]^T$
Multiplication	$ab = \left[a_0 b_0 - \bar{a} \cdot \bar{b}, \left(a_0 \bar{b} + b_0 \bar{a} + \bar{a} \times \bar{b}\right)^T\right]^T$
Scaler Multiplication	$\lambda a = \left[\lambda a_0, \lambda \bar{a}^T\right]^T$
Dot Product	$a \cdot b = a_0 b_0 + \bar{a} \cdot \bar{b}$
Conjugate	$a^* = \left[a_0, -\bar{a}^T\right]^T$
Norm	$\|a\| = \sqrt{a \cdot a}$
Inverse	$a^{-1} = \frac{a^*}{\|a\|^2}$

Table 1. Quaternion Operations $(\mathbb{H})$

Equation (6) and (13) will now be mapped from $\mathbb{R}^3$ to $\mathbb{H}$ (where $\mathbb{H}$ denotes quaternion space) since quaternion algebra will be advantageous when solving for $\left(\bar{a}^B_{B/I}\right)_{drag}$. In this case, mapping $\mathbb{R}^3$ to $\mathbb{H}$ is as simple as rewriting the variables in $\mathbb{R}^3$ as vector quaternions (scaler part zero). For example, this means that a variable $\bar{x} \in \mathbb{R}^3$ will be mapped into $\mathbb{H}$ as $x = \left[0, \bar{x}^T\right]^T \in \mathbb{H}$. Referring to the canonical quaternion operations presented in Table 1 and setting,

$$q_{\mathcal{H}} = \begin{bmatrix} 0 \\ \left[\left(I^{TM}\right)^{-1} - \left(I^B\right)^{-1}\right] \mathcal{H}\left(I^B, \Delta\bar{x}_{TM,B}\right) \end{bmatrix} \quad \text{and} \quad q_{drag} = \begin{bmatrix} 0 \\ m^B \left(I^B\right)^{-1} \bar{x}_{Cp/B} \end{bmatrix}$$

yields the translational and angular relative acceleration measurement equations in $\mathbb{H}$,

$$a^B_{TM/B} = \left(a^B_{TM/I}\right)_{Earth} - \left(a^B_{B/I}\right)_{Earth} - \left(a^B_{B/I}\right)_{drag} + \left(a^B_{TM/B}\right)_{other} \tag{14}$$

$$\alpha^B_{TM/B} = q_{\mathcal{H}} \left(a^B_{TM/I}\right)_{Earth} - q_{\mathcal{H}} \left(a^B_{B/I}\right)_{Earth} - q_{drag} \left(a^B_{B/I}\right)_{drag} + \left(\alpha^B_{TM/B}\right)_{other} \tag{15}$$

Between Eq. (14) and Eq. (15) there appears to be three unknowns: $\left(a^B_{TM/I}\right)_{Earth}$, $\left(a^B_{B/I}\right)_{Earth}$ and $\left(a^B_{B/I}\right)_{drag}$. However, if $\left(a^B_{TM1/I}\right)_{Earth}$ is solved for in Eq. (15) and plugged into Eq. (14), $\left(a^B_{B/I}\right)_{Earth}$ will cancel out. Therefore, there are two equations with two unknowns. From Eq. (14) and Eq. (15) the drag acting on the spacecraft may now be solved for directly,

$$\begin{aligned} \left(a^B_{B/I}\right)_{drag} = \left(q^{-1}_{\mathcal{H}} q_{drag} - 1_q\right)^{-1} \Big[& a^B_{TM/B} - q^{-1}_1 \alpha^B_{TM/B} + q^{-1}_1 \left(\alpha^B_{TM/B}\right)_{other} \\ & - \left(a^B_{TM/B}\right)_{other} \Big] \end{aligned} \tag{16}$$

Here, 1_q denotes the unit quaternion $1_q = [1, 0, 0, 0]^T \in \mathbb{H}$, and x^{-1} denotes the quaternion inverse acting on a variable $x \in \mathbb{H}$ and is presented in Table 1.

SIMULATIONS

Using Eq. (1) the torques acting on the GRACE-FO spacecraft and the S-GRS's test mass were modeled in MATLAB for a near polar nadir-pointing orbit assuming a known gravitational potential. The moment of inertia of the GRACE-FO spacecraft was acquired from the GRACE-FO user handbook[10] while the moment of inertia of the S-GRS's test mass was acquired from Álvarez et al.[5] The MATLAB function *gravitysphericalharmonic* was used to find the translational accelerations from Earth's gravitational potential field for zonal spherical harmonic degrees $n = 1, 2, ..., 23$. Then $\bar{a}_{J_1}, \bar{a}_{J_2}, ..., \bar{a}_{J_{23}}$ were plugged into Eq. (2) to calculate $G_{J_1}, G_{J_2}, ..., G_{J_{23}}$, respectively, for both the spacecraft and the test mass. Next, $G_{J_1}, G_{J_2}, ..., G_{J_{23}}$ were plugged into Eq. (1) to acquire the gravity-gradient torques acting on the spacecraft and test mass. Figure 3 presents the angular acceleration sensitivity of the S-GRS (solid black line) compared to the relative angular acceleration amplitude spectral density between the GRACE-FO spacecraft and the S-GRS's test mass. The angular acceleration sensitivity of the S-GRS was calculated from the S-GRS's transitional acceleration sensitivity simulations.[5] Figures 4 through 7 present the S-GRS's sensitivity to the individual zonal spherical harmonics.

The nongravitational accelerations from the Level-1B GRACE-FO data products[14] were then applied to the GRACE-FO spacecraft in addition to the gravity gradient torque and translational gravitational acceleration for zonal spherical harmonic degrees $n = 1, 2, ..., 23$. Equations (10) and (16) were used to solve directly for the drag acting on the GRACE-FO spacecraft with the results presented in Figure 8 and Figure 9, respectively.

DISCUSSION

From Figures 4 through 7 it is proven that the S-GRS will be able to measure to the relative gravity-gradient torque between the spacecraft and test mass resulting from zonal spherical harmonic order 23 or higher. However, the main take away from these figures is not the order of zonal spherical harmonic degree which will be observable, instead the main take away is that the relative gravity-gradient torque will be observable at all to the S-GRS's accelerometer. This is important since as previously stated, the relative gravity-gradient induced torque data is not currently utilized for the GRACE-FO data products which is attributed to limitations with the current ONERA accelerometers.[4]

Since the accelerometer in the S-GRS will be sensitive to the relative gravity-gradient induced torque, the algorithm derived in Eq. (16) may be utilized to directly measure the drag acting on the spacecraft with a single S-GRS accelerometer. Directly measuring drag is of critical necessity since drag modeling errors are a main contributor of error in the current version 04 release of the GRACE-FO data products.[8,9] Additionally, when we compare the results of the algorithm in Eq. (16) to the results of the algorithm presented in Eq. (10) we find both errors to be on the order of $\approx 10^{-13}$ m/s^2. This result is greatly important for future gravity recovery missions since instead of requiring a minimum of two precision accelerometers to directly measure drag, only a single S-GRS is needed.

Finally, it is important to note that for the simulations which estimated the drag acting on the spacecraft in Figures 8 and 9, the terms which subtract out additional external forces $\left(\alpha^{B}_{TM1/B}\right)_{other}$ and $\left(a^{B}_{TM1/B}\right)_{other}$, were set to zero. Both terms were set to zero because the algorithm directly solves for the drag (i.e. no estimation nor filtering), therefore the accuracy of the drag estimation becomes a function of the modeling accuracy of the other nongravitational forces

(Solar radiation pressure, Earth radiation pressure, spacecraft - test mass coupling, etc.), which may be modeled more accurately than the drag acting on the spacecraft.[9] Therefore, modeling and adding the other external forces to the spacecraft - test mass system only to then subtract them out directly in Eq. (10) and Eq. (16) would be a null point for these simulations.

CONCLUSIONS

This research formulated the gravity-gradient torque equations for zonal spherical harmonic order n when Earth's gravitational potential is known. This research also proved that the S-GRS will be sensitive to the gravity-gradient induced torques acting on its test mass through simulations which plotted the relative angular acceleration amplitude spectral density between the GRACE-FO spacecraft and the S-GRS's test mass. The newly-available measured relative angular accelerations between the gravity recovery spacecraft and test mass were then used to directly measure the drag acting on a gravity recovery spacecraft with only a single S-GRS accelerometer. This algorithm was then compared to the another drag estimation algorithm which requires a minimum of two accelerometers. Through this comparison, it was shown that the both algorithms are able to estimate the drag to a similar error level. Finally, to the extent of the authors' knowledge, this research is novel since no other research has investigated the sensitivity of precision accelerometers to gravity gradient induced torque, nor has any research demonstrated the potential for these measurements to improve the accuracy of gravity recovery mission observables.

REFERENCES

[1] M. v. d. Meijde, R. Pail, R. Bingham, and R. Floberghagen, "GOCE data, models, and applications: A review," *International Journal of Applied Earth Observation and Geoinformation*, Vol. 35, Mar. 2015, pp. 4–15, 10.1016/j.jag.2013.10.001.

[2] S. Cesare, "PERFORMANCE REQUIREMENTS AND BUDGETS FOR THE GRADIOMETRIC MISSION," *Thales Alenia Space*, Vol. 14, No. 01, 2008.

[3] N. Harvey and C. Sakumura, "Results from a GRACE/GRACE-FO attitude reconstruction Kalman filter," *Journal of Geodesy*, Vol. 93, Sept. 2019, pp. 1881–1896, 10.1007/s00190-019-01289-z.

[4] N. Harvey, C. M. McCullough, and H. Save, "Modeling GRACE-FO accelerometer data for the version 04 release," *Advances in Space Research*, Vol. 69, Feb. 2022, pp. 1393–1407, 10.1016/j.asr.2021.10.056.

[5] A. D. Álvarez, A. Knudtson, U. Patel, J. Gleason, H. Hollis, J. Sanjuan, N. Doughty, G. McDaniel, J. Lee, J. Leitch, S. Bennett, R. Bevilacqua, G. Mueller, R. Spero, B. Ware, P. Wass, D. Wiese, J. Ziemer, and J. W. Conklin, "A simplified gravitational reference sensor for satellite geodesy," *Journal of Geodesy*, Vol. 96, sep 2022, p. 70, 10.1007/s00190-022-01659-0.

[6] R. Bernknopf, D. Brookshire, Y. Kuwayama, M. Macauley, M. Rodell, A. Thompson, P. Vail, and B. Zaitchik, "The Value of Remotely Sensed Information: The Case of a GRACE-Enhanced Drought Severity Index," *AGU Fall Meeting 2019*, Vol. 10, AGU, American Meteorological Society, jan 2018, pp. 187–203, 10.1175/wcas-d-16-0044.1.

[7] N. R. Council *et al.*, *Satellite gravity and the geosphere: contributions to the study of the solid Earth and its fluid envelopes*. National Academies Press, 1997.

[8] R. P. Kornfeld, B. W. Arnold, M. A. Gross, N. T. Dahya, W. M. Klipstein, P. F. Gath, and S. Bettadpur, "GRACE-FO: The Gravity Recovery and Climate Experiment Follow-On Mission," *Journal of Spacecraft and Rockets*, Vol. 56, may 2019, pp. 931–951, 10.2514/1.a34326.

[9] S. Behzadpour, T. Mayer-Gürr, and S. Krauss, "GRACE Follow-On Accelerometer Data Recovery," *Journal of Geophysical Research: Solid Earth*, Vol. 126, May 2021, p. e2020JB021297, 10.1029/2020jb021297.

[10] H. Y. Wen, G. Kruizinga, M. Paik, F. Landerer, W. Bertiger, C. Sakumura, T. Bandikova, and C. Mccullough, "Gravity recovery and climate experiment follow-on (GRACE-FO) level-1 data product user handbook," *JPL D-56935 (URS270772)*, Vol. 11, 2019.

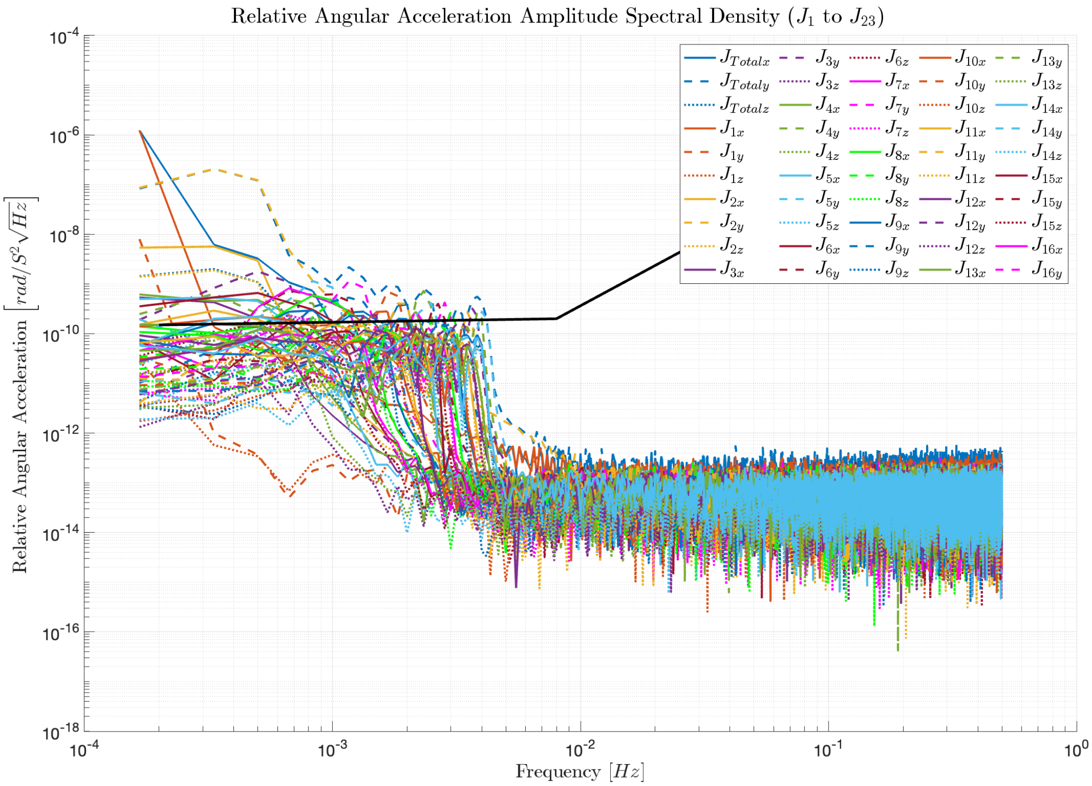

Figure 3. Relative Angular Acceleration Amplitude Spectral Density Between the GRACE-FO Spacecraft and The S-GRS's Test Mass for Zonal Spherical Harmonic Degrees J_1 to J_{23}.

[11] F. L. Markley and J. L. Crassidis, *Fundamentals of Spacecraft Attitude Determination and Control*. Springer New York, 2014, 10.1007/978-1-4939-0802-8.

[12] P. Chen, X. Sun, and C. Han, "Gravity Gradient Tensor Eigendecomposition for Spacecraft Positioning," *Journal of Guidance, Control, and Dynamics*, Vol. 38, Nov. 2015, pp. 2200–2206, 10.2514/1.g001195.

[13] N. Brandt and W. Fichter, "Revised electrostatic model of the LISA Pathfinder inertial sensor," *Journal of Physics: Conference Series*, Vol. 154, mar 2009, p. 012008, 10.1088/1742-6596/154/1/012008.

[14] NASA Jet Propulsion Laboratory (JPL), "GRACE-FO Level-1B Release version 4.0 from JPL in ASCII," 2019, 10.5067/GFL1B-ASJ04.

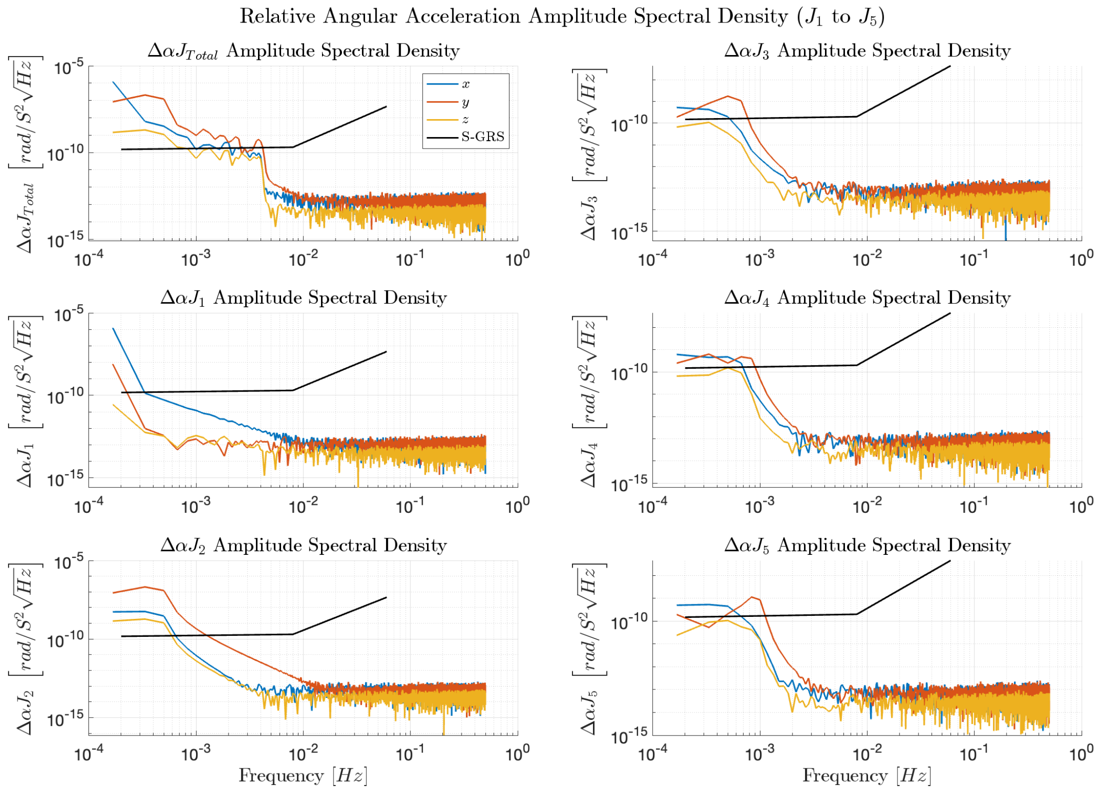

Figure 4. Relative Angular Acceleration Amplitude Spectral Density Between the GRACE-FO Spacecraft and The S-GRS's Test Mass for Zonal Spherical Harmonic Degrees J_1 to J_5.

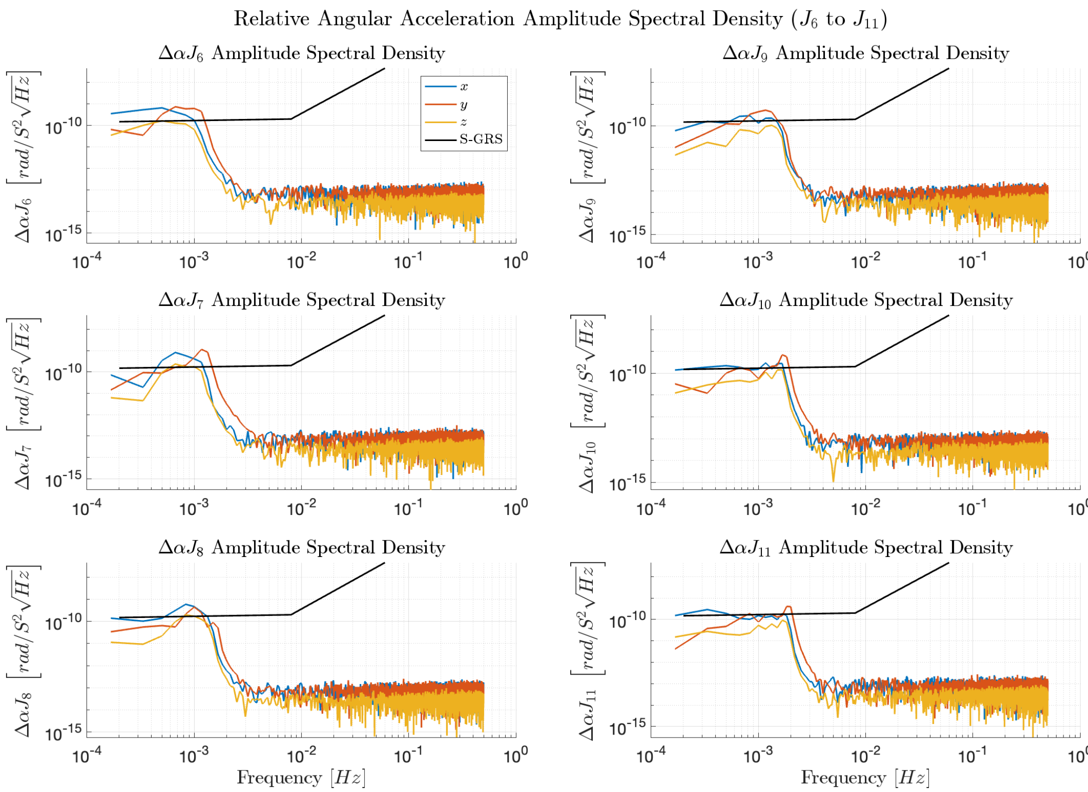

Figure 5. Relative Angular Acceleration Amplitude Spectral Density Between the GRACE-FO Spacecraft and The S-GRS's Test Mass for Zonal Spherical Harmonic Degrees J_6 to J_{11}.

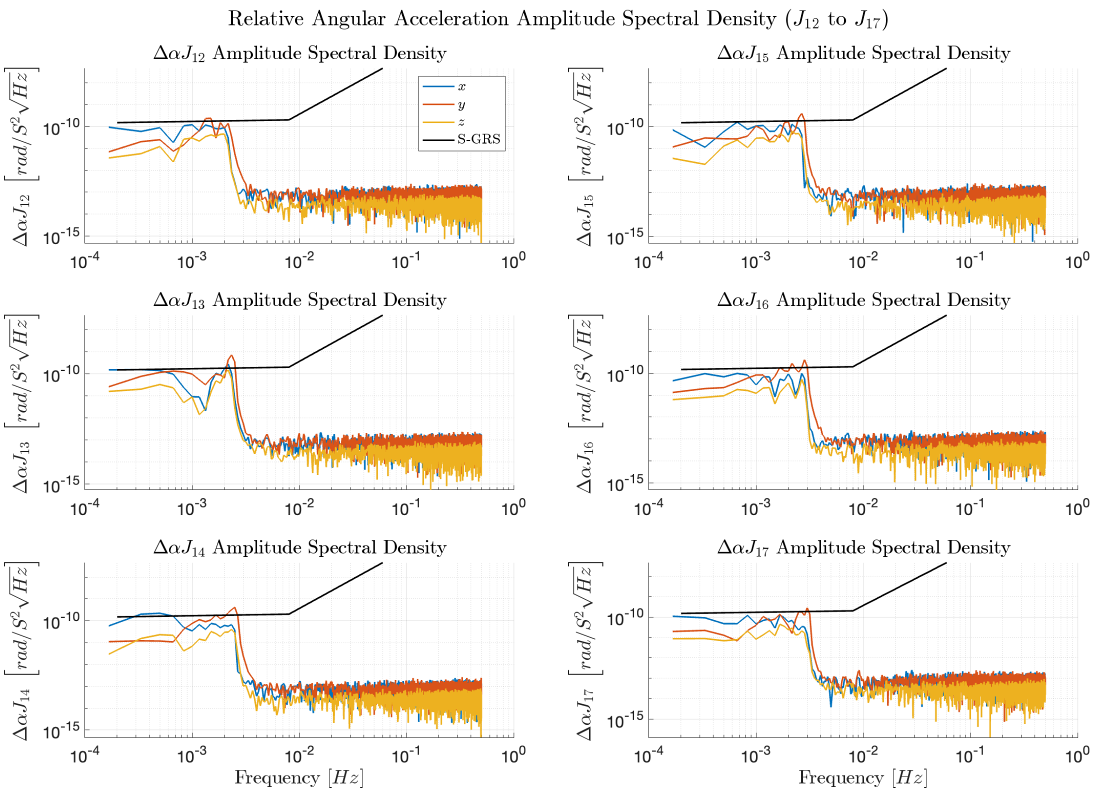

Figure 6. Relative Angular Acceleration Amplitude Spectral Density Between the GRACE-FO Spacecraft and The S-GRS's Test Mass for Zonal Spherical Harmonic Degrees J_{12} to J_{17}.

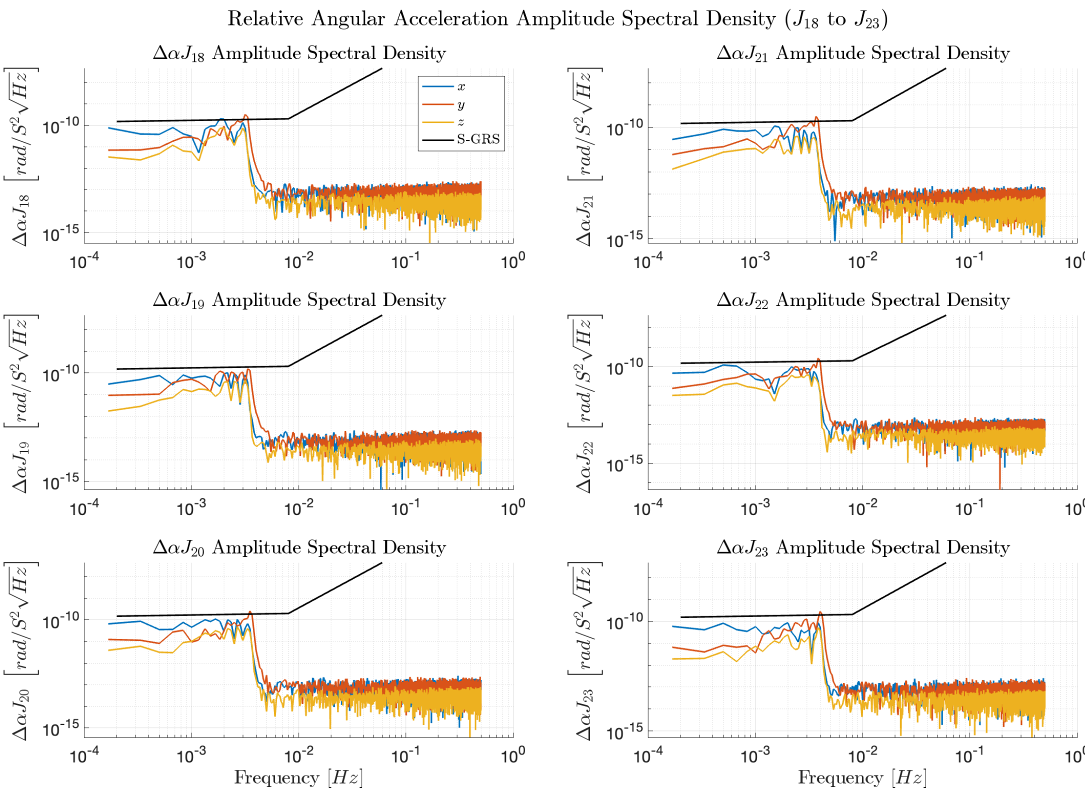

Figure 7. Relative Angular Acceleration Amplitude Spectral Density Between the GRACE-FO Spacecraft and The S-GRS's Test Mass for Zonal Spherical Harmonic Degrees J_{18} to J_{23}.

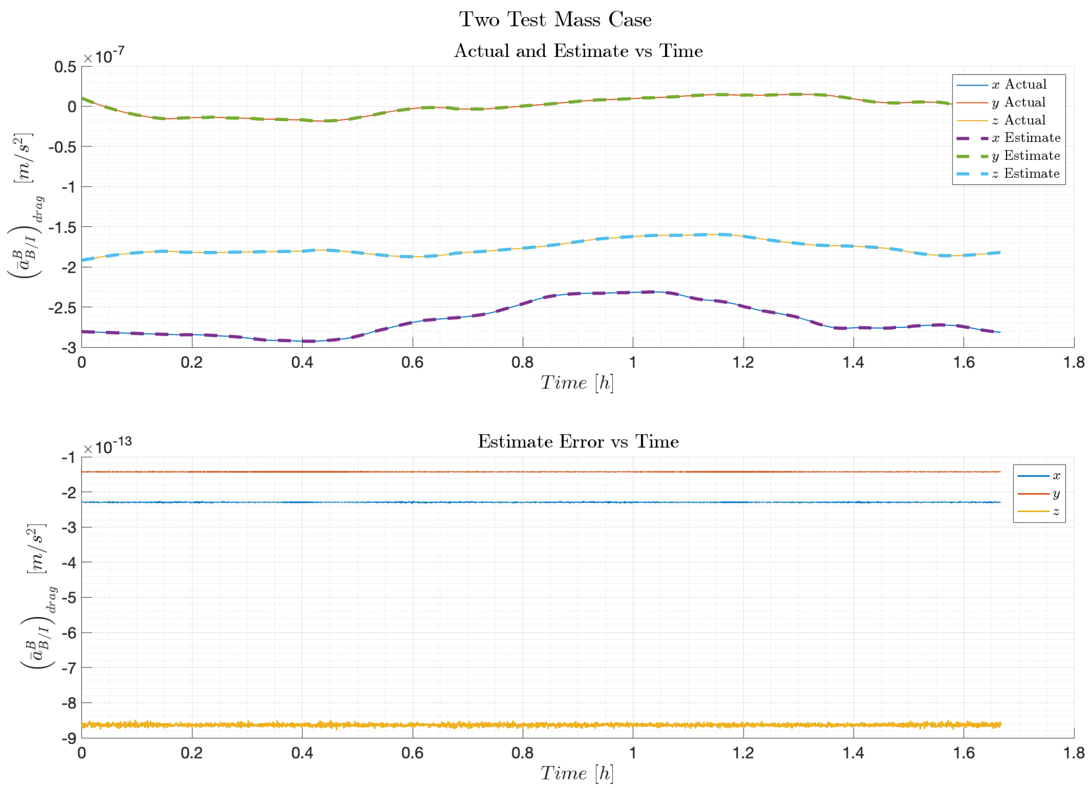

Figure 8. Two Test Mass Estimation Case

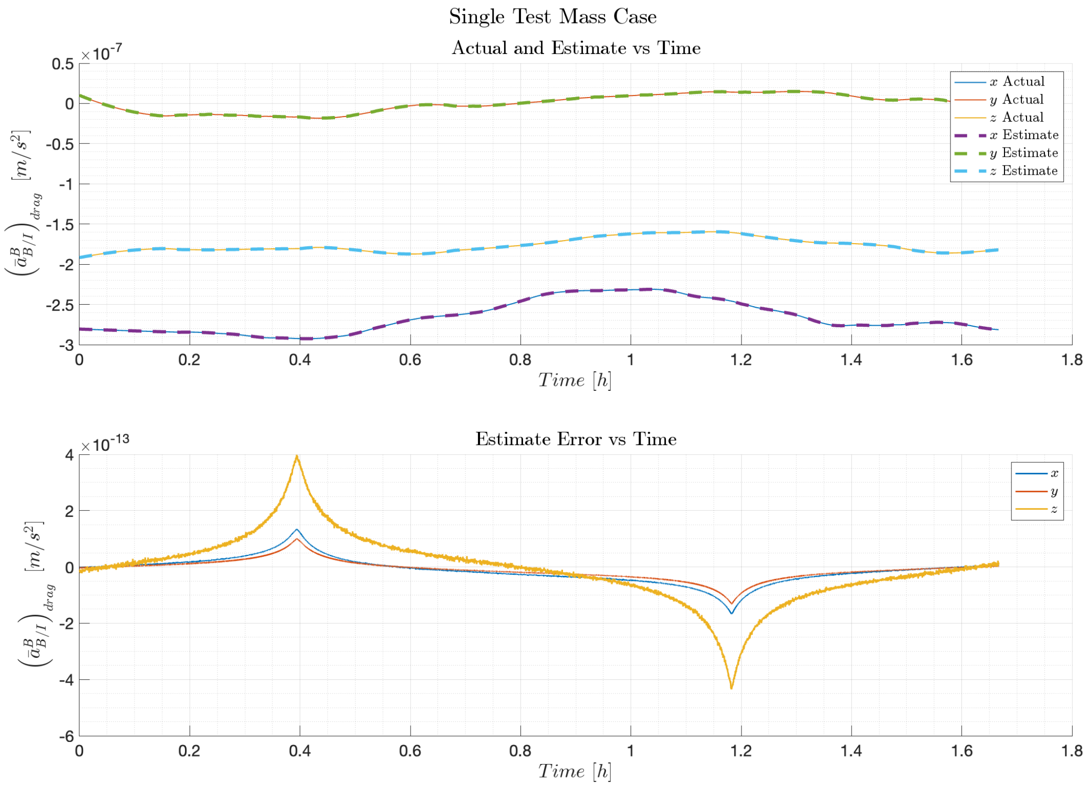

Figure 9. Single Test Mass Estimation Case